Insulators Backflashover Caused by Lightning Strokes Along the Span

Gonçalo Inácio, goncalo.inacio@tecnico.ulisboa.pt
Instituto Superior Técnico, Universidade de Lisboa, Av. Rovisco Pais, 1049-001 Lisboa, Portugal

***Abstract*— One of the main causes of power supply interruptions is the lightning strokes incidence along the overhead transmission lines. The performance of the line against lightning strokes terminating to towers or shield wires is accounted by the backflashover rate (BFR).**

The BFR is commonly calculated by considering the lightning strokes terminating to shield wires along the span by using a span factor (or reduction factor) of 0,6. This coefficient is used since the overvoltage at the tower decreases by comparison with the overvoltage caused by a stroke terminating to tower. Recent studies refer that the use of this coefficient may lead to underestimate the backflashover rate.

It is developed a simulating Monte Carlo procedure that is applied to determine the span factor. The simulation algorithm is built at MATLAB and the lightning stroke incidence at the transmission line is simulated with EMTP program.

The results indicate that the use of the span factor 0,6 might lead to underestimating the backflashover rate calculated for the transmission lines reproduced in this work, especially for higher ground resistance values and in cases that the line presents a worse performance.

Deterministic simulations are performed to identify the influence that the lightning stroke terminating point and the ground resistance value have on the backflash occurrence possibility. It is observed that for terminating points more distance from the tower the decrease in the backflash occurrence possibility, when compared with a stroke direct to tower, is less pronounced for ground resistance higher values.

***Index Terms:* BFR, backflashover, EMTP, lightning stroke, Monte Carlo, span factor**

I. INTRODUCTION

The BFR is traditionally calculated by (1), this method is recommended by CIGRE [1] and comes from Hileman's studies at [2].

$$\mathrm{BFR} = 0{,}6 \times \mathrm{N_L} \times P(\mathrm{I_c}) \qquad (1)$$

where $\mathrm{N_L}$ is the expected number of strikes to 100 km of the line and $P(\mathrm{I_c})$ is the probability of a lightning strokes to exceed the critical current $\mathrm{I_c}$ that leads line insulator to flashover.

The span factor is used since the overvoltage originated in the insulator is higher for a stroke that terminates on tower, compared with terminate along the span.

Recent studies reveal that this methodology, when considering the effect of distribution of strokes along the span through the suggested span factor, may underestimate the calculation of BFR. According to S. Visacro et al. [3] and Z. G. Datsios et al. [4] the value of the span factor to be used in the calculation of the BFR may vary: between 0.81 and 0.94 and between 0.5 and 0.9, respectively.

The objective of this work is to estimate the span factor using the Monte Carlo method, by comparing the distributed incidence of strokes in the line with the concentrated incidence of strokes to tower. The modelling of the discharge current and the different components of the line is done in the EMTP program, and the simulation algorithm is created in MATLAB.

II. SYSTEM MODELING AND METHOLOGY

A. Simulated system characteristics

The simulated system is shown in Figure 1. The system is reproduced considering five towers of a 150 kV line, delimiting four spans with a length of 300 meters.

The lightning stroke is simulated through a current source, each span of the line is represented by a transmission line of frequency-dependent parameters, and the equivalent of the network is represented by a voltage source. To avoid reflections from the terminating line connections, it is added a line with a very high length (50 km), maintaining the characteristics of the conductors.

To distribute the incidence of strokes along the line, the span between Tower 2 and Tower 3 is sectioned into line segments 30 meters long, thus six lightning incidence points are considered (between support 3 and the half span).

The tower is modeled by dividing it into segments and the insulator simulation is based on the leader progression model. It is considered that all towers are connected to the earth through a resistance, that simulates the ground electrode.

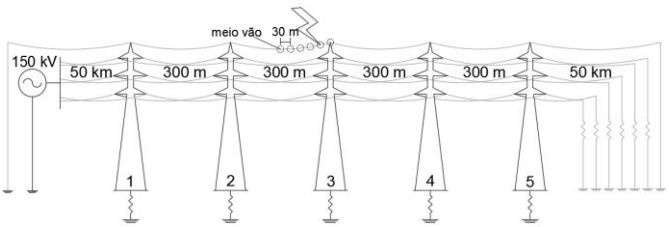

Figure 1. Simulated system representation.

Current and voltage measurements are made on Tower 3. The EMTP returns to each simulation the values of current and voltage with time, Figure 2 shows the current and voltage measurements made on one of the tower arms, where I is the current at the tower arm and $\mathrm{U_C}$ is the voltage at the insulator.

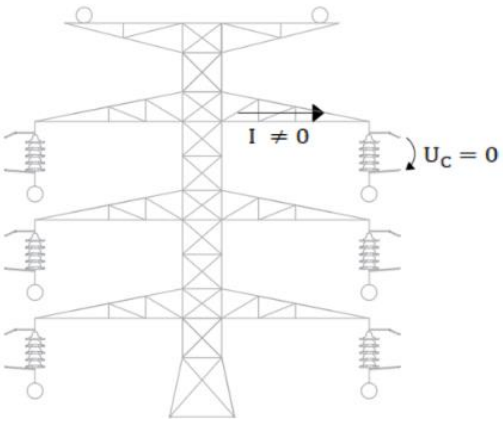

Figure 2. Representation of current and voltage measurements.

B. Monte Carlo procedure

The flowchart of the Monte Carlo procedure in Figure 3 identifies the functioning of the simulation algorithm adopted in this work. Where N_{it} is the algorithm number of iterations and N is the number of the simulation in progress.

On each iteration, is defined the random variables, and the simulation in EMTP is performed only after verifying if the peak current value of the stroke is enough to be attracted by the shield wires. The algorithm also collects the simulation results to identify the occurrence of flashovers.

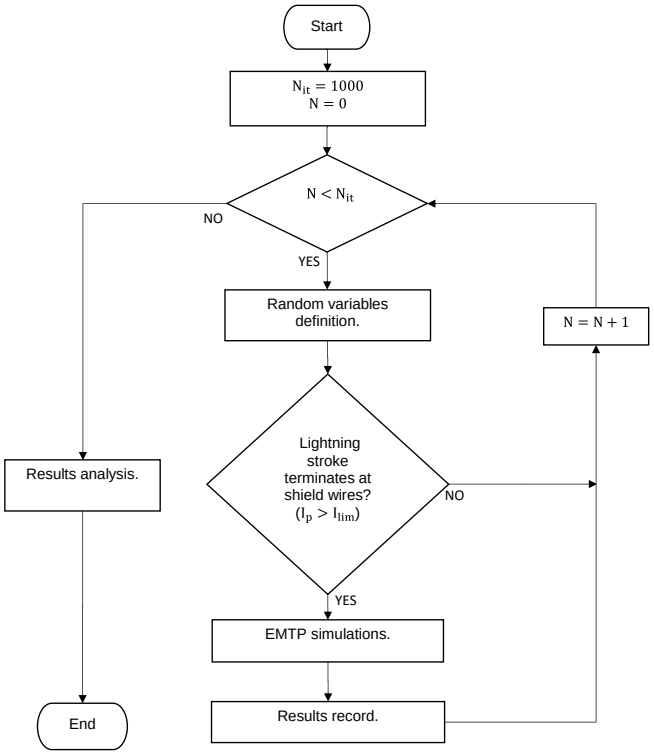

Figure 3. Flowchart of Monte Carlo procedure.

The random simulation variables generated are the lightning stroke current parameters, the voltage phase, the terminating point of the stroke and the ground resistance.

The lightning stroke current parameters that characterize his waveform obey to a log-normal distribution so that to apply the Monte Carlo method it is necessary to transform this distribution into a normal distribution (logarithmic transformation). The expressions (2), (3), (4), (5) and (6) show this transformation by applying a variable change, which allows to obtain the expression used to randomly determine the value of each parameter.

$$P(X) = \int_{-\infty}^{X} \left[\frac{1}{\sqrt{2\pi}\,\beta x} \, e^{-\left(\frac{z^2}{2}\right)} \right] dx \tag{2}$$

$$z = \frac{\ln\left(\frac{x}{M}\right)}{\beta} \tag{3}$$

making variable change $x' = z$

$$P(X') = \int_{-\infty}^{X'} \left[\frac{1}{\sqrt{2\pi}} \, e^{-\left(\frac{x'^2}{2}\right)} \right] dx' \tag{4}$$

A random number is generated between 0 and 1 for (x') and using (5), you get (X').

$$X' = P^{-1}(X') = \sqrt{2} \times \text{erfinv}(2x' - 1) \tag{5}$$

As z = X', the value for a given parameter (x) is found by (6)

$$z = \frac{\ln\left(\frac{x}{M}\right)}{\beta} \Leftrightarrow x = M \cdot e^{\beta z} \tag{6}$$

The lightning stroke current simulation parameters are the peak current (I_p), the rise time ($t_{d30/90}$) and the maximum steepness of the front (Sm). The values of the median (M) and standard deviation (β) recommended by CIGRE [5], used in the (6) for the calculation of each the parameters mentioned are defined in Table 1.

Table 1. Log-normal distribution parameters for lightning stroke simulated current

Parameter	M	β
I_p [kA]	31,10	0,484
$t_{d30/90}$ [kA/µs]	3,83	0,553
S_m [µs]	$3{,}9 \times I_p^{\,0{,}55}$	0,599

The value for the voltage phase is randomly generated in each iteration, varying between 0º and 360º.

When considering simulations with distributed incidence, the terminating point is determined considering that all points have the same probability, since it is considered an equivalent geometry in which the air conductors are in parallel with the ground.

The ground resistance value can be defined as a value that remains constant in all simulations or be defined using the probabilistic distribution determined based on real values. The distribution of ground resistance values is presented in Figure 4. The mean value resistance of the probabilistic distribution,

which is equal to 16.16 Ω.

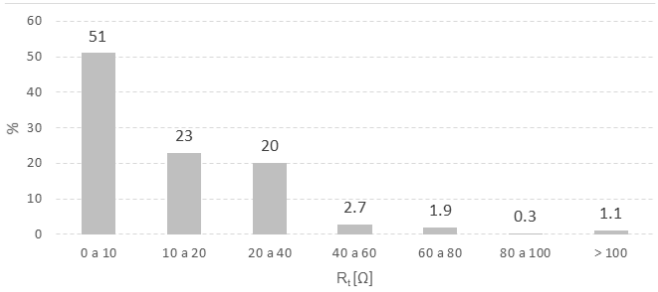

Figure 4. Grounding resistance distribution.

To account only strokes that strike the shield wires and the tower, during the algorithm is calculated the limit current of shielding failure (depends on the geometry of the support). For current values higher than the limit current of shield failure the phases are protected.

The value of I_{lim} is obtained by applying the Pythagoras theorem to the diagram in Figure 5, which represents the perfect shielding situation by using the Modified Electrogeometric Model, obtaining (7).

Expression (7) relates the height, and the distance between the conductors with the attractive radius that lead to the perfect shielding situation. Where h_G is the height of the shield wire, h_F is the height of the phase conductor and d_h is the horizontal distance between the shield wire and the phase conductor. The value of the limit current of shielding failure is determined by the equation system composed by (7), (8) and (9). Where R_{ac} is the shield wire attractive radius, and R_{ag} is the phase conductor attractive radius.

$$(d_h + R_{ac})^2 = -(h_G - h_F)^2 + {R_{ag}}^2 \Leftrightarrow R_{ac} = \sqrt{{R_{ag}}^2 - (h_G - h_F)^2} - d_h \quad (7)$$

$$R_{ag} = 0{,}67{h_G}^{0,6}{I_{lim}}^{0,74} \quad (8)$$

$$R_{ac} = 0{,}67{h_F}^{0,6}{I_{lim}}^{0,74} \quad (9)$$

When it is verified that the generated stroke strikes the shield wires the program modifies the corresponding simulation file and starts the simulation with the variables determined in this iteration of the algorithm.

The simulations are carried out to reproduce situations in which the strokes have incidence considered as: concentrated on tower and distributed along the span.

The insulator flashover leads to the existence of current between the air gap, and since the arc voltage is not considered, it will correspond to a zero voltage at the insulator (as in Figure 2). Thus, to confirm the existence of backflashover in the simulation, the EMTP program returns to the MATLAB the voltage measured at the insulator and the current at the tower arms.

When the measured current is different from zero, it means the existence of insulator backflashover. The occurrence backflashover is also verified by a consecutive measurement of voltages different from zero.

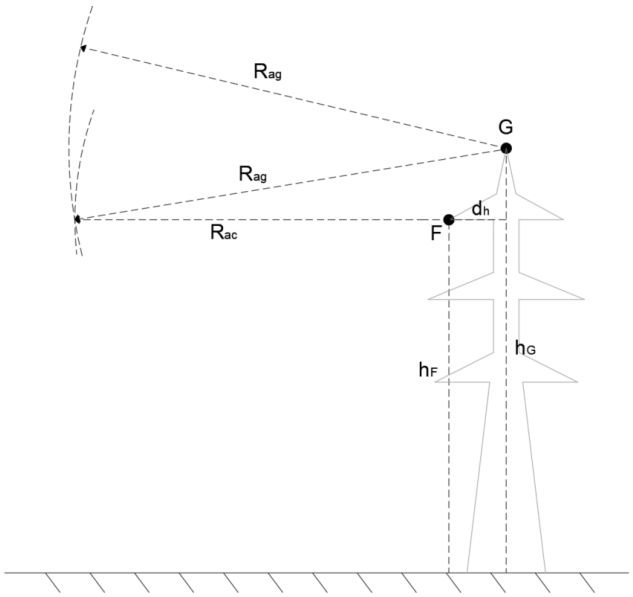

Figure 5. Perfect shielding situation by using the Modified Electrogeometric Model

After the total number of iterations, the algorithm counts the number of flashovers observed and estimates BFR and span factor. Given the analysis made in [6], considering 1000 and 5000 simulations, there was no significant difference in the results obtained, as such it is used 1000 iterations.

The BFR, which represents the number of lightning strokes, per 100km of line and per year, that terminates at shield wires or at tower, and lead to the insulator flashover, is calculated by the (10) and (11). Where BFR_C is the backflashover rate considering concentrated incidence of strokes to tower and BFR_D is the backflashover rate considering distributed incidence of strokes to the shield wires and tower. The total number of iterations (N_{it}) corresponds to the number of lightning strokes considered.

$$BFR_C = N_L \times \frac{Nc}{N_{it}} \quad (10)$$

$$BFR_D = N_L \times \frac{Nd}{N_{it}} \quad (11)$$

The annual number of lightning strokes to the line per 100 km (N_L) is determined by (12), obtained by using the Modified Electrogeometric Model. Where it depends on the height of the shield wire (h_G), the horizontal distance between the shield wires (d_h) and the current value (I_{med}). The height of the shield wire and the distance between shield wires and phase conductor depends on the geometry of the line. According to the recommendations of the IEEE [7], the current value used (I_{med}) corresponds to the average value of the simulated currents, determined from the peak current values. It is considered a 0,7-ground flash density, per year and per km^2.

$$N_L = 0{,}1 \times 0{,}7 \times (2 \times (0{,}67 \times h_G^{0,6} \times {I_{med}}^{0,74}) + s) \quad (12)$$

The span factor (FR) (13) is determined by the ratio between the number of flashovers observed by the distributed incidence of strokes by the shield wires and the number of flashovers originated by the concentrated incidence of strokes at tower. This ratio relates BFR_D with BFR_C.

$$FR = \frac{BFR_D}{BFR_C} \quad (13)$$

C. Models for network components

C1. Lightning stroke

The lightning stroke is represented by the CIGRE concave current source. The parameters received by EMTP are described in Figure 6, extracted from the program. As mentioned at Table 1, the parameters are the peak current (I_p), the rise time ($t_{d30/90}$) and the maximum steepness of the front (Sm), (the first two are represented respectively at the figure as I_{max} and t_f,).

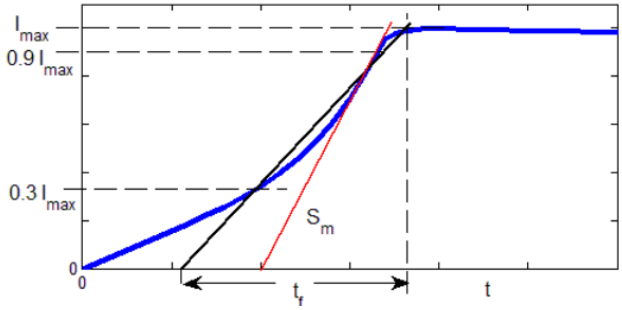

Figure 6. Simulated lightning stroke current waveform.

C2. Transmission line

The line is simulated by the J. Marti [8] model already implemented in EMTP. This model uses a real and constant frequency transformation matrix, maintaining the frequency dependence of longitudinal line parameters. On the admittance matrix parameters calculation, the capacitance of the line is defined as constant, which leads to neglect the corona effect that occurs in the existence of an imperfect dielectric.

To characterize the line in the simulation model it is necessary to define the geometry of the line and the conductor's cables characteristics.

C3. Tower

The model is based on the multistory transmission tower model, proposed by Ishii et al. [9], and consists of the use of an ideal transmission line (of constant parameters) representing the structure of the tower between the lower arms and the ground resistance, and the remaining sections are represented by an equivalent inductance of 1 μH per unit of length, as in Figure 7 (whose configuration will correspond to one of the case studies).

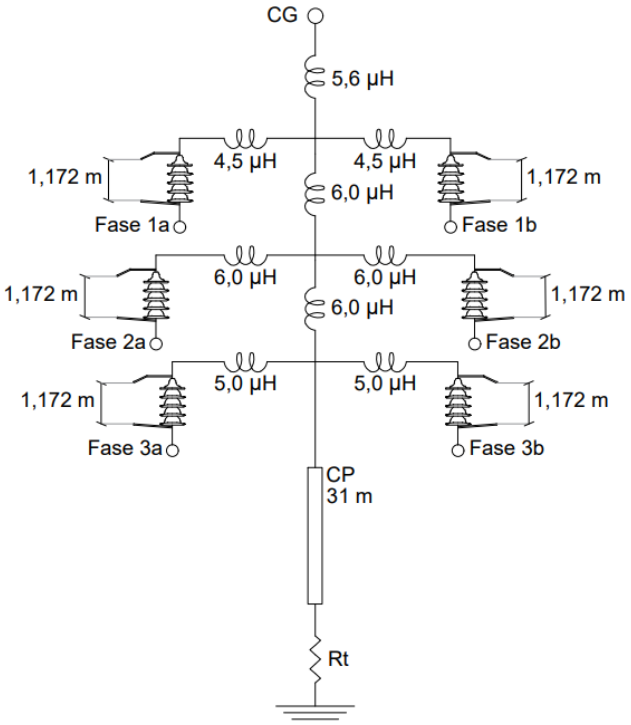

Figure 7. Tower, insulators, and ground resistance representation.

C4. Insulators

The insulators are simulated by the model available in EMTP, which is based on the leader progression model. In this model it is assumed that the flashover mechanism always consists of three phases: corona inception, streamer propagation and leader progression.

The total time for flashover occurrence (t_c) can be expressed as (14).

The time for corona inception (t_i), considering that the applied voltage presents high rising rate, can be disregarded.

The streamer propagation (t_s), which represents about 30 % of the total time, depends on the polarity and waveform applied, as well as the geometry of the electrodes [1]. Given the difficulty in modeling it, this time is usually not considered.

$$t_c = t_i + t_s + t_l \quad (14)$$

The leader progression time (t_l) is calculated based on the determination of the leader velocity (v_l), as shown in (15). Which depends on the voltage across the gap u(t), the leader length l_l, the gap length d_G, and on the constants k and E_o which depends on the insulator type and electrode configuration.

$$\frac{dl}{dt} v_l = k \cdot u(t) \left[\frac{u(t)}{d_G - l_l} - E_o \right] \quad (15)$$

C5. Ground electrode

The ground electrode is represented in a concentrated and linear way by the ground resistance (R_t on Figure 7). Thus, it is made a conservative analysis, since the soil ionization is not considered.

III. APPLICATIONS

A. Practical cases

Three case studies are analyzed based on the configurations of the 150kV transmission lines used in Portugal. The general characteristics of the line common to the three cases are summarized in Table 2.

It is considered a length span of 300 meters, a sag (distance between maximum and minimum height of the span) of 6,324 meters and a gap length of 1,172 meters at the insulators.

Table 2. Line characteristics.

Voltage	150 kV
Span	300 m
Sag	6,324 m
Gap length	1,172 m

A1. Case A

In the study case A is reproduced a double circuit line with one shield wire. The tower geometry is represented in Figure 8.

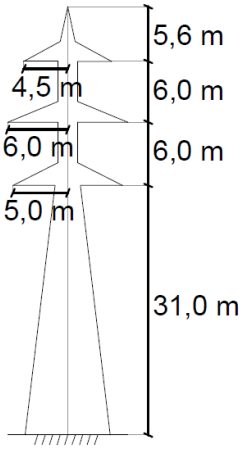

Figure 8. Tower geometry for case A.

The phase conductor and the shield wire characteristics correspond to the aluminum-steel cables habitually used in Portugal, called BEAR and SWG 19/13, respectively. The characteristics of the conductors are in Table 3.

Table 3. Phase conductor and shield wire characteristics, case A.

	Cable	**R_{DC} [Ω/km]**	**D [cm]**	**SE**
Phase conductor	BEAR	0,112	2,345	0,286
Shield wire	SWG 19/13	1,82	1,17	0,2

A2. Case B

In study case B is reproduced a double circuit line with two shield wires. The tower geometry is represented in Figure 9.

The configuration of the line results from the remodulation of the line of study case A. With the installation of a second shield wire aims to improve its performance by reducing the number of incidents.

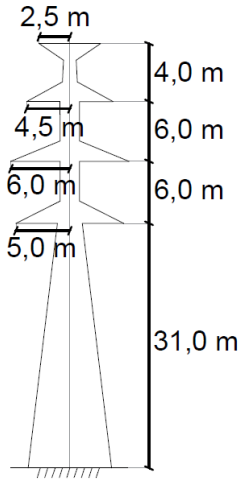

Figure 9. Tower geometry for case B.

The phase conductor characteristics remain in relation to case A and the shield wire used correspond to the conductors commonly referred to as GUINEA and OPGW. The conductor characteristics used to reproduce the line of case B are summarized in Table 4.

Table 4. Phase conductor and shield wire characteristics, case B and case C.

	Cable	**R_{DC} [Ω/km]**	**D [cm]**	**SE**
Phase conductor	BEAR	0,112	2,345	0,286
Shield wire	GUINEA	0,359	1,46	0,2
	OPGW	0,288	1,625	

A1. Case C

In study case C, is reproduced a simple line with two shield wires. The tower geometry is shown in Figure 10.

The characteristics of phase conductors and guard cables are the same as in case study B (Table 4).

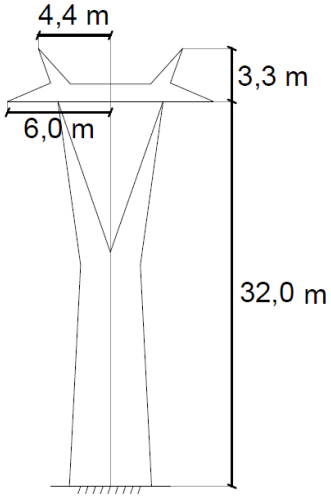

Figure 10. Tower geometry for case C.

B. Deterministic simulations

B1. Ground resistance influence

Lightning strokes terminating to tower are simulated for different ground resistivity values and are obtained: the time evolution of the current flowing to the ground and the time evolution of the voltage originated in the insulator (Figure 11).

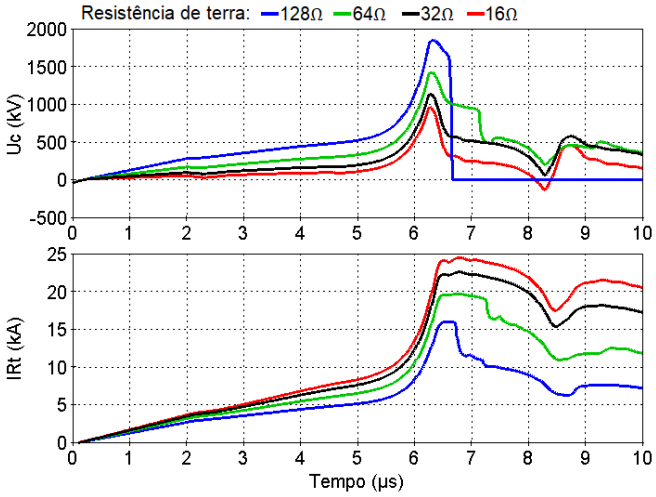

Figure 11. Time evolution of the current flowing to the ground, and of the voltage at the insulator string, for different values of R_t.

The Table 5 summarizes the values obtained in the simulations performed. The results obtained are as expected, as observed by the increase of the voltage at the insulator string and the decrease at the current measured. These variations occurs when the ground resistivity increases.

This increase of the voltage can also be observed for other terminating points in Figure 12. The terminating points considered are: at tower, 30 meters, 90 meters, and 150 meters.

For terminating points more distant from the tower it is predicted that the decrease in the possibility of flashover is less pronounced for higher resistance values.

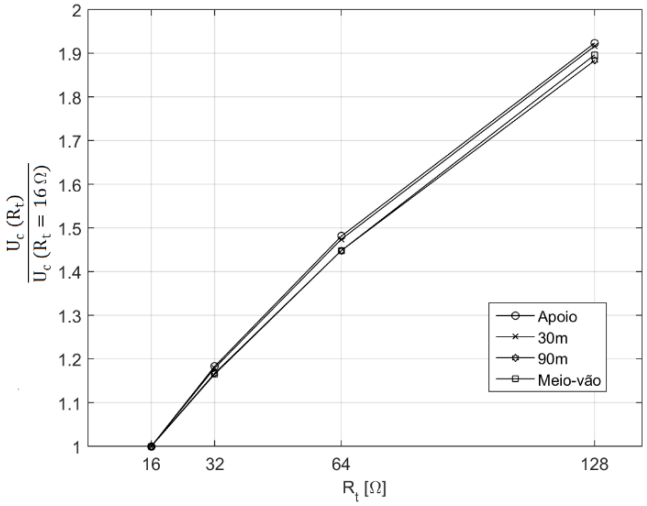

Figure 12. Increase of the peak voltage with the value of the ground resistance.

Table 5. Maximum values of voltage and current measured.

R_t [Ω]	$I_{Rt}(R_t)$ [kA]	$\frac{I_{Rt}(R_t)}{I_{Rt}(R_t = 16\,\Omega)}$	$U_C(R_t)$ [kV]	$\frac{U_C(R_t)}{U_C(R_t = 16\,\Omega)}$
16	24,53	1	960,34	1
32	22,59	0,92	1135,99	1,18
64	19,69	0,80	1422,42	1,48
128	16,02	0,65	1846,42	1,92

B2. Terminating point influence

From Figure 13 is observed a decrease in the peak current when the point of incidence moves away from the support for different values of ground resistance.

These results confirm that the decrease of the peak current is less pronounced for higher ground resistance values.

For R_t=16 Ω, the peak current after a strike terminate at mid span is about 0.79 times the value of the peak current the discharge terminates at tower. Considering R_t=128 Ω this ratio is about 0.88.

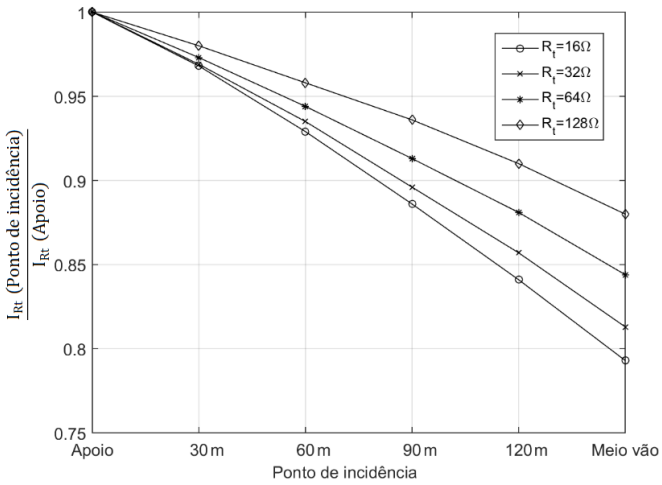

Figure 13. Peak current variation with the stroke terminating point.

At Figure 14, when it's considered an R_t=16 Ω shows the decrease of the peak voltage originated at the insulator string with the increase of the terminating point distance. This decrease is shown in the three phases. In this case, phase 2 is always more prone to occur flashover.

The decrease that occurs in the current and in the voltage observed with the increase of the terminating point distance, can be explained by the influence of the reflections existing on the adjacent tower. When traveling a longer distance to the tower, the current is more subject to the losses existing in the line.

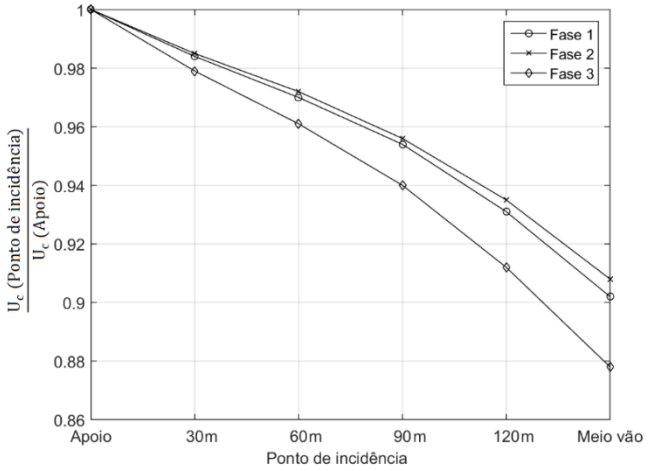

Figure 14. Decrease of the peak voltage at the insulator string with the increase of the terminating point distance.

B3. Reflections from adjacent tower

To visualize the influence of the existing reflections on the adjacent tower in the reduction of the overvoltage originated in the insulator string, simulations were performed considering a span with a length of 50 km, thus preventing the reflections from contributing to the overvoltage attenuation.

Figure 15 shows the time evolution of the voltage with and without the contribution of reflections from the adjacent tower, considering that the stroke terminates to tower. There is a reduction of about 5% of the peak voltage at the insulator string.

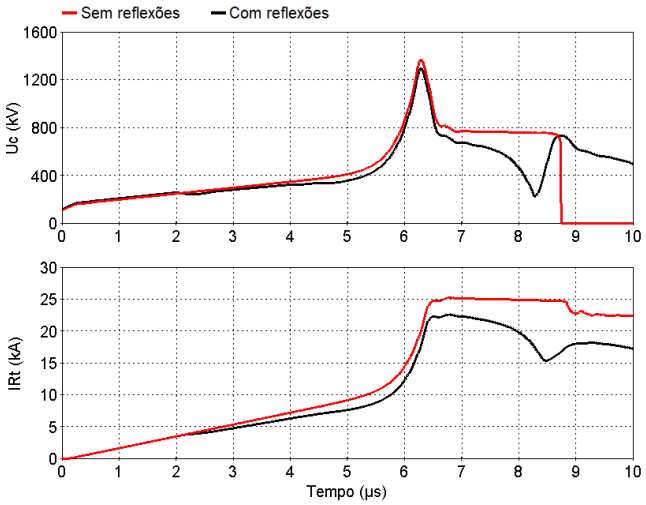

Figure 15. Time evolution of voltage and current with and without reflections from adjacent tower. Strokes terminating to tower.

Figure 16 shows the time evolution of the voltage across the insulator, with and without the contribution of reflections in the adjacent tower, considering that the stroke terminates 150 meters from tower. It is found a reduction of about 15% of peak voltage at the insulator string.

These results show that the existing reflections in the line have a significant contribution in the influence that the strike terminating point has on the occurrence of backflashover.

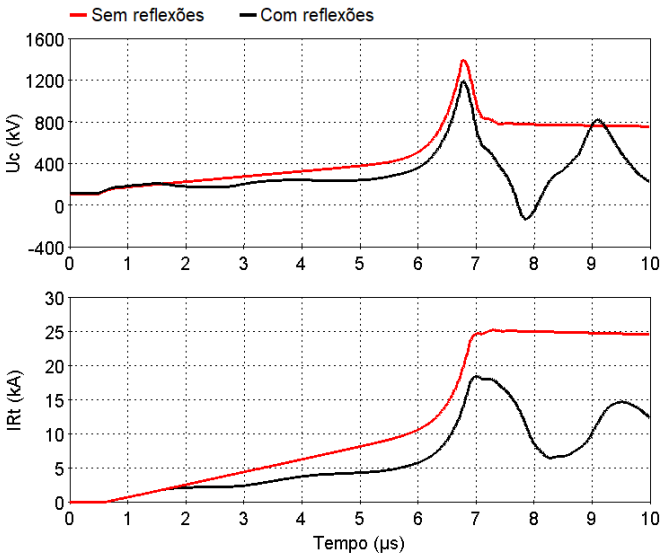

Figure 16. Time evolution of voltage and current, with and without reflections from adjacent tower. Strokes terminating to mid span.

B4. Critical current

Figure 17 shows the increase of the critical current value with the increase of the distance from the strike terminating point, considering different values of the ground resistance. Considering the value of the ground resistance equal to 16 Ω, it is observed that the critical current for a strike terminating to mid span has increased about 2 times the critical current determined for the stroke terminate tower. Considering ground resistance of 128 Ω, this ratio is about 1.2.

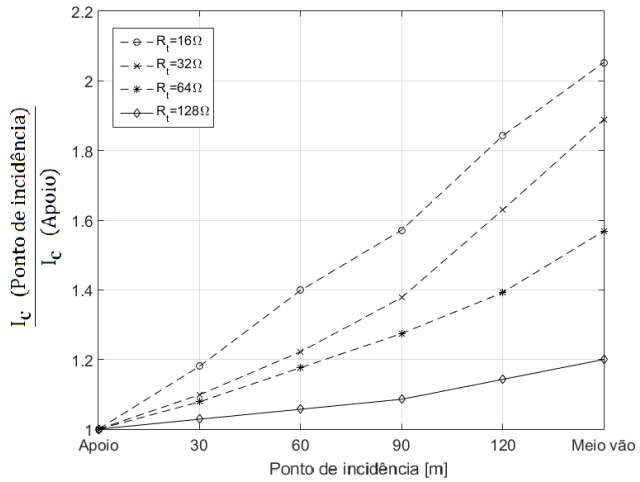

Figure 17. Increase of the critical current with the stroke terminating point for different resistance values.

The results obtained indicate that the variation strike terminating point contributes significantly to the possibility of backflashover depending on the value of the ground resistance. Being expected that for higher ground resistance values the value of the reduction factor will be higher.

III. RESULTS

The Monte Carlo procedure implemented allows to estimate the span factor for each study case.

As indicated by the deterministic analysis, different values of ground resistance result in different values of the span factor. As so, span factor is estimated for 16 Ω, 32 Ω, 64 Ω, 128 Ω and with the probabilistic method that determines the resistance value in each simulation. For each study case are obtained the following results:

- Limit current of shielding failure (I_{lim});
- Backflahsover rate when considering all strokes terminating at tower (BFR_D);
- Backflahsover rate when considering all strokes terminating at tower (BFR_C);
- Number of flashovers observed when considering stroke incidence distribuited along the span (N_D);
- Number of flashovers observed when considering all strokes terminating at tower (N_C);
- Span factor (FR).

A1. Case A

In case A the limit current of shielding failure is 21.57 kA, and 791 of the 1000 strokes analysed strikes the shield wires or tower.

The results observed in the Monte Carlo simulations are found in Table 6.

Table 6. Monte Carlo simulations results for case A.

R_t	N_D	N_C	BFR_D	BFR_C
16 Ω	54	76	0,74	1,04
32 Ω	219	323	3,01	4,44
64 Ω	502	618	6,90	8,49
128 Ω	718	765	9,87	10,51
Prob.	96	111	1,32	1,53

A2. Case B

In case A the limit current of shielding failure is 11.88 kA, and 980 of the 1000 strokes analyzed strikes the shield wires or the tower.

The line reproduced in case of study B results from the remodeling of the line reproduced in case A to improve its performance, this improvement is reflected in the reduction that occurs in the estimated values of the backflashover rate.

The results observed in the Monte Carlo simulations are found in Table 7.

Table 7. Monte Carlo simulations results for case B.

R_t	N_D	N_C	BFR_D	BFR_C
16 Ω	15	18	0,21	0,25
32 Ω	73	100	1,01	1,38
64 Ω	229	310	3,17	4,29
128 Ω	441	508	6,10	7,02
Prob.	33	40	0,46	0,55

A3. Case C

In case C the limit current of shielding failure is 3,14 kA, and all strokes analyzed strikes the shield wires or the tower.

As expected, the reproduced line performs better than the previous ones. For lower ground resistance values there is a small number of flashovers and the use of the probabilistic distribution of ground resistance values don't lead to any flashover.

The results observed in the Monte Carlo simulations are found in Table 8.

Table 8. Monte Carlo simulations results for case C

R_t	N_D	N_C	BFR_D	BFR_C
16 Ω	1	3	0.01	0.03
32 Ω	19	38	0,20	0,40
64 Ω	96	131	1,02	1,39
128 Ω	237	294	2,52	3,13
Prob.	0	0	0	0

A4. Results analysis

The results are considered unreliable when the number of backflashover observed for strokes concentrated at tower (N_D) is less than 100. Thus, Table 9 presents the estimate of the span factor for the values of ground resistance of 32 Ω, 64 Ω and 128 Ω for cases A and B, and 64 Ω and 128 Ω for case C.

The results indicate that the span factor tends to increase with the increase in the value of the ground resistance and that differs according to the geometry of the line, ranging in case A between 0.68 and 0.97, in case B between 0.73 and 0.87 and in case C between 0.73 and 0.81.

Although the mean value of the probabilistic distribution of ground resistance is 16.16 Ω, the estimated reduction factor for case A is 0.86. This indicates that the flashovers that occur when the ground resistance has higher values have a higher preponderance.

Table 9. Span factor found for case A, B and C.

R_t	Fator de Redução		
	A	B	C
32 Ω	0,68	0,73	-
64 Ω	0,81	0,74	0.73
128 Ω	0,97	0,87	0.81
Prob.	0,86	-	-

It is verified that the influence of backflashover originated by discharges along the span in reducing the value of the BFR (when considering concentrated incidence in support) is more pronounced for lines that present better performance.

The use of the reduction factor 0.6 would lead to underestimating the calculation of the BFR of the cases studied, especially for higher ground resistance values, that is, in cases with worse performance.

III.CONCLUSION

The analytical procedures, used to determine the way of calculating the BFR proposed by Hileman, consider the various factors that influence the probability to occur flashover by a stroke terminating to shield wire. Still, analytical analysis leads to the use of simplified models. [2]

In this work a computational program was developed that through Monte Carlo simulations determines the span factor by comparing the incidence strokes distributed along the span and the incidence strokes concentrated in tower. The simulation algorithm was developed in MATLAB and the simulation of the incidence of lightning stroke in the line is performed in the EMTP program.

In addition, deterministic simulations were performed to identify the parameters that have a greater contribution in reducing the BFR.

The main conclusions from the results obtained are:

• For striking points more distant from the tower, the decrease in the possibility of flashover is less pronounced for higher ground resistance values;

• The reflections existing in the line have a significant contribution in the influence that the stroke striking point has on the possibility of backflashover;

• The influence of the stroke terminating along the span in reducing the BFR is more pronounced for lines that present better performance (depends on the characteristics of the line);

• The use of the reduction factor 0.6 may lead to underestimating the BFR calculation, especially for higher ground resistance values, that is, in cases with worse performance.

REFERENCES

[1] CIGRE WG 01 SC33, "Guide to procedures for estimating the lightning performance of transmission lines," in *Brochure 63*, 1991.

[2] A. R. Hileman, Insulation Coordination for Power Systems, 1999.

[3] S. Visacro, F. H. Silveira, R. M. Gomes e R. S. Ono, "The Impact of the Distribution of Lightning Strikes along the Span on Backflashover Rate of Transmission Lines," in *34th International Conference on Lightning Protection (ICLP)*, 2018.

[4] Z. G. Datsios, P. N. Mikropoulos, T. E. Tsovilis, V. T. Karakostas e S. P. Mavidou, "Estimation of the Minimum Backflashover Current of 150 and 400 kV Overhead Transmission Lines Through ATP-EMTP Simulations: Effect of the Lightning Stroke Location Along Line Spans," in *21st International Symposium on High Voltage Engineering (ISH)*, 2019.

[5] CIGRE WG C4.407, "Lightning Parameters for Engineering Applications," in *Brochure 549*, 2013.

[6] A. M. Chagas, "Estudo do Desempenho de Linhas de Transmissão de Energia Face a Descargas Atmosféricas por Simulações de Monte Carlo," in *Dissertação Mestrado, Instituto Superior Técnico, Universidade de Lisboa*, 2017.

[7] IEEE Std 1243-1997, "IEEE Guide for Improving the Lightning Performance of Transmission Lines," in *IEEE Working Group on the Lightning Performance of Distribution Lines*, 1997.

[8] J. Marti, "Accurate Modeling of Frequency Dependent Transmission Lines," in *IEEE Transactions on Power Apparatus and Systems, Vol. PAS-101, pp. 147-155*, January 1982.

[9] M. Ishii, T. Kawamura, T. Kouno, E. Ohsaki, K. Murotani and T. Higuchi, "Multistory transmission tower model for lightning surge analysis," in *IEEE Trans. on Power Delivery, vol. 6, no. 3, pp. 1327-1335*, July 1991.